An optimal arrangement of mooring lines for the three-tether submerged point-absorbing wave energy converter

N.Y. Sergiienko[a,*], B.S. Cazzolato[a], B. Ding[a], M. Arjomandi[a]

[a] *The University of Adelaide, School of Mechanical Engineering, Adelaide, Australia*

Abstract

Point-absorbing wave energy converters (WECs) with a single-tether mooring are capable of extracting power from heave motion, but they do not utilise the full energy harvesting potential. One of the possible ways to increase the total power absorption is to add another controllable degree of freedom. These can be achieved by using a so-called 'tripod' configuration when the body is tied to three tethers attached to the power take-off systems at the sea floor. This paper investigates the optimal inclination of tethers considering two different approaches: a purely kinematic analysis, not taking into account the shape of the buoy and a dynamic analysis of spherical and cylindrical WECs, using a linear frequency-domain method. The results show that for a submerged sphere and for a submerged vertical cylinder with an aspect ratio of one, tethers should be orthogonal to each other, forming edges of the cuboidal vertex. Such a configuration of tethers provides for uniform performance of the WEC in all directions of motion. However, for the cylinders with an aspect ratio other than one, an optimal angle between the tethers depends greatly on the ratio between the cylinder height and diameter.

Keywords: Wave energy, wave energy converter, submerged point absorber, three-tether mooring

1. Introduction

Ocean waves are a huge resource of renewable energy with great potential to be captured and employed for electricity generation and water desalination. Many concepts for extracting energy from surface waves have been realised, leading to more than 200 different wave energy converters (WECs) in various stages of development [1]. Despite the wide variety of WECs technologies on offer, floating and fully submerged point absorbers comprise a great proportion of existing full-scale prototypes of WECs, which typically operate in deep water waves with high energy content [2]. In most cases, a point absorber, whose dimensions are smaller than a wavelength, is designed as an axisymmetric buoy with the main advantage being insensitive to wave direction [3].

An axisymmetric body as a prospective WEC has been thoroughly studied in [4, 5, 6], showing that its maximum power absorption is independent of the scale of the device and is a function of the wavelength of an incident wave and oscillatory modes of the body. The majority of existing point-absorbing WECs operate only in the heave mode, limiting energy extraction to approximately one third of the available energy [7]. Such considerable attention to the heaving buoys can be explained by the relative simplicity of the design and the lower capital cost as compared with WECs with multiple degrees of freedom. However, a point absorber that oscillates in two modes (heave/surge or heave/pitch) with optimal control parameters can theoretically capture three times more power than a heaving device, achieving the maximum power absorption for such types of WECs [7].

Depending on the power take-off (PTO) operating principle and type of mooring configuration, existing WECs with multiple degrees of freedom can be divided into two categories (similar to the classification in [8]):

(i) WECs that utilise slack mooring lines just to keep a body on site (Figure 1a). Such mooring configurations are not involved in power generation and have been applied to the floating WECs, such as SEAREV [9] or Pelamis [3]. The power take-off system of these devices is located inside the buoy's hull, that can impose constraints on the size of the system.

(ii) Floating or fully submerged energy converters where the mooring legs are always under tension (Figure 1b). In this configuration, tethers can be attached through spools to the electrical generators, as is implemented in the 3D-WEC that is under development by Resolute Marine Energy, Inc. [10], or to a piston of a hydraulic PTO system. A solo-duck WEC, developed by The University of Edinburgh [11], can also be classified in this category.

Although the effect of slack mooring lines on the performance of the floating WECs has been assessed in [12,

*Corresponding author

Email address: nataliia.sergiienko@adelaide.edu.au (N.Y. Sergiienko)

Nomenclature

A	amplitude of the incident wave
$\mathbf{A}, \mathbf{B}$	hydrodynamic added mass and damping coefficient matrix
$\mathbf{F}_{exc}$	incident wave excitation force
$\mathbf{F}_{pto}$	force exerted on the WEC due to the power take-off system
$\mathbf{F}_{rad}$	hydrodynamic radiation force
G	buoy centre of mass
H	WEC (cylinder) height
$\mathbf{I}_3$	identity matrix of size 3×3
$\mathbf{J}^{-1}, \bar{\mathbf{J}}^{-1}$	inverse kinematic Jacobian of the WEC: conventional and dimensionally homogeneous
N_i, L_i	attachment points of the i-th tether to the buoy hull and sea floor respectively
$\mathbf{N}_0, \mathbf{S}_0$	skew-symmetric matrices that represent $[\mathbf{n}_0]_\times^\intercal$ and $[\mathbf{s}_0]_\times^\intercal$ respectively
P	WEC power absorbed
T	dynamic tension in the tether
$\mathbf{Z}_{buoy}, \mathbf{Z}_{pto}$	hydrodynamics impedance of the buoy and impedance of the PTO system
a	WEC radius
$c_t, \mathbf{C}_t, \tilde{\mathbf{C}}_t$	power take-off damping: coefficient, matrix for one tether and a collective matrix for all tethers
$\mathbf{e}_{si}$	unit-vector directed along i-th tether
$\mathbf{f}_t$, τ_t,	force and torque applied from the tether to the buoy
d_s	submergence depth of the WEC (distance from the sea water level to the WEC centre of mass)
g	gravitational acceleration
h	water depth
k	wavenumber ($\omega^2 = gk \tanh kh$)
$k_t, \mathbf{K}_t, \tilde{\mathbf{K}}_t$	power take-off stiffness: coefficient, matrix for one tether and a collective matrix for all tethers
l_i	dynamic length of the i-th mooring line
$m_b, \mathbf{M}$	WEC mass and mass matrix
m_w	mass of water displaced by the WEC
$\mathbf{n}_i$	position vector of the i-th tether attachment point relative to the buoy centre of mass
$\mathbf{q}$	vector of three leg length variables
$\mathbf{r}$	vector of linear displacements of the WEC
$\mathbf{s}_i$	vector directed along i-th tether
$\mathbf{x}$	6 DoF WEC position vector
α	inclination angle of each tether to the vertical
$\delta(\cdot)$	change in vector or scalar from nominal position
γ_0	distribution of the tether tension force over its length
κ	condition number
ω	radial wave frequency
ρ	water density
θ	angle between two tethers in the plane that they form
ϑ	vector of angular displacements of the WEC

13, 14], a mooring configuration with tethers under tension is of more practical interest for submerged buoys due to the required positive buoyancy of the WEC.

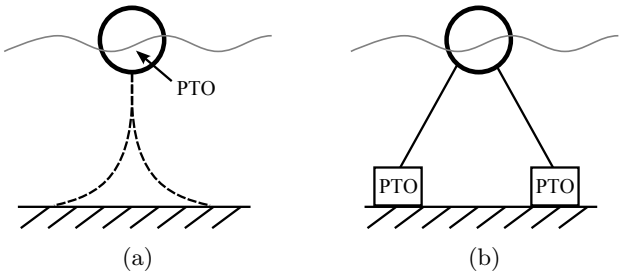

Figure 1: A schematic representation of mooring configurations: (a) slack mooring lines, (b) tension leg moorings.

An axisymmetric body needs to oscillate in two modes (radiating symmetric and antisymmetric waves) to absorb the maximum available energy [7]. Even though a body is symmetrical about a vertical axis, the addition of mooring lines makes the whole system asymmetric and therefore sensitive to the direction of wave propagation. This means that a WEC should oscillate along the vertical axis (heave) radiating symmetric waves, and in a horizontal plane (surge-sway or pitch-roll) radiating antisymmetric waves along the axis aligned with the propagation of incident waves. Having three motion modes that need to be controlled, intuitively, the minimum number of tethers in a mooring configuration is also three. Moreover, hydrodynamic forces that act on the axisymmetric body are uncoupled for surge, sway and heave, but are coupled for surge/pitch and sway/roll motions [7]. Therefore, ideally, the mooring design should not impose additional coupling

between modes.

A system with a three-cable mooring of a submerged sphere was first proposed in [15]. The configuration, where three cables are equally inclined to the vertical and situated symmetrically around a sphere, provides an independence of surge, sway and heave motions, while all three modes are dependent on the parameters of a power take-off system and an inclination angle of cables [15]. Wave-to-wave tuning of the PTO parameters is an objective of a WEC control system, whereas the inclination angle of the cables cannot be changed during the life-span of the device and should be optimised during the design stage to maximise energy harvesting. However, the system in [15] was explored with only two inclination angles of the cables: 45 and 60 degrees, and the dependence of the power absorption on the angle has not yet been explored. A similar tripod WEC design has been used as a benchmark device in [10, 16] to test a developed optimal causal control system. This WEC consists of a floating cylinder attached to three tethers that are inclined to the vertical by 63.5 degrees, which seems to have been chosen arbitrarily by the researchers. To the best knowledge of the authors, these studies are the only ones that have considered a WEC with multiple degrees of freedom using a three-leg mooring. Consequently, the question of an optimal mooring configuration that maximises absorbed power remains open and is discussed in this paper.

In this research, the tripod system is investigated for a fully submerged point-absorbing WEC, similar to the CETO system developed by Carnegie Wave Energy Limited [17]. Section 2 studies the problem from the kinematics point of view without taking into account any hydrodynamic properties of the WEC. Next, an optimal mooring configuration is examined for two generic buoy shapes: a sphere and a vertical cylinder, employing hydrodynamic models that are derived by using a linear wave theory approximation. The dynamic analysis in Section 3 is performed in the frequency domain, assuming a linear time-invariant system, an ideal control system and small displacements of the buoy, as compared with the length of the mooring lines. Results in Section 3 demonstrate the sensitivity of the optimal tether inclination angle to the number of parameters, such as the submergence depth of the WEC, sea site water depth, mass of the buoy, wave direction, body aspect ratio and a set of control parameters. Finally, the effect of the tether configuration on power generated by the WEC is investigated in Section 4.

2. Kinematic analysis

In this section, the kinematics of the system is studied to provide an understanding of the optimal arrangement of tethers from a kinetic energy transmission and controllability point of view.

A thorough analysis of any mechanism, including wave energy converters, starts from kinematics [18]. For the analysis of existing WEC devices, the kinematics only shows the relationship in coordinates and velocities between moving and fixed parts of the system. However, in the conceptual design stage, a kinetostatic analysis answers several important questions, such as: (i) how the small changes in the buoy position (velocity) relate to changes in the tether length (velocity) and vice versa [19]; (ii) how force and torque loads on the body affect the tension forces in the mooring lines and how these forces are distributed between all tethers; (iii) how many motion modes can be controlled using a specific mooring configuration (controllability analysis) [20].

From the kinematic point of view, the current WEC system shares similarities with parallel mechanisms, also referred to as parallel robots (Figure 2), where the buoy acts as an end-effector and tethers play the role of actuated joints/legs (Figure 3). It is assumed that tethers are connected to the ocean floor and to the buoy hull through the spherical joints. Such a configuration, 3-SPS (spherical-prismatic-spherical), has 6 degrees of freedom [21] and 3 actuators, meaning that this system is under-actuated.

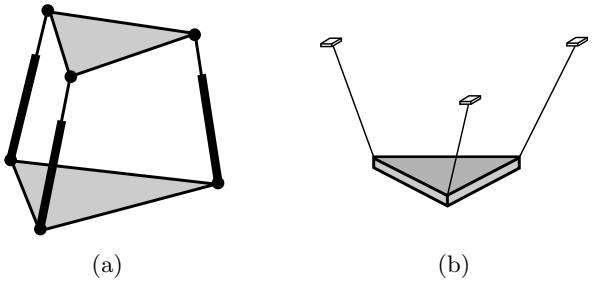

Figure 2: A schematic representation of parallel robots: (a) 3-SPS parallel mechanism; (b) cable driven parallel robot with three cables.

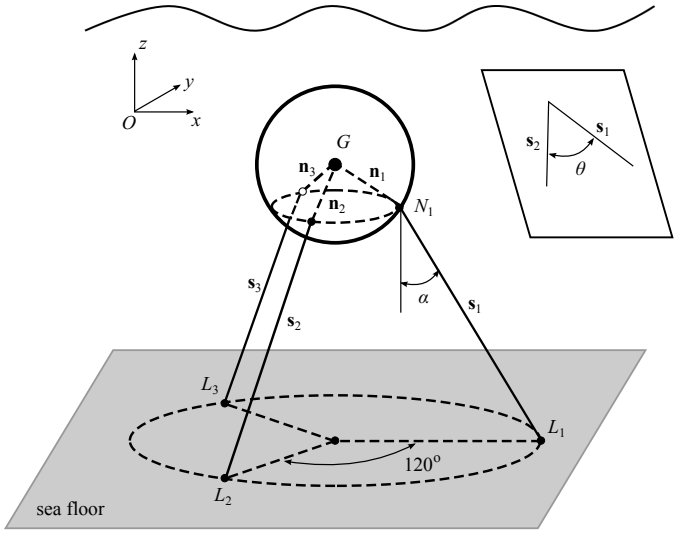

Figure 3: The arrangement of mooring lines around a submerged WEC. Adapted from [10].

Optimal design methodologies of parallel robots rely on the forward and inverse kinematic analysis of mechanisms using Jacobian and inverse Jacobian matrices [21].

The kinematic Jacobian provides mapping from actuated joint velocities to the end-effector velocities in a Cartesian coordinate frame. However, for parallel robots it is easier to derive an analytical form of the inverse kinematic Jacobian [22], which is:

$$\dot{\mathbf{q}} = \mathbf{J}^{-1}\dot{\mathbf{x}}, \tag{1}$$

where $\mathbf{x} = [\mathbf{r} \quad \vartheta]^\intercal$ is an end-effector location vector with three translational and three rotational motions, $\mathbf{q} = [l_1 \quad l_2 \quad l_3]^\intercal$ is a vector of three leg length variables and an inverse kinematic Jacobian $\mathbf{J}^{-1}$ can be obtained as

$$\mathbf{J}^{-1} = \begin{pmatrix} \mathbf{e}_{s1}^\intercal & (\mathbf{n}_1 \times \mathbf{e}_{s1})^\intercal \\ \mathbf{e}_{s2}^\intercal & (\mathbf{n}_2 \times \mathbf{e}_{s2})^\intercal \\ \mathbf{e}_{s3}^\intercal & (\mathbf{n}_3 \times \mathbf{e}_{s3})^\intercal \end{pmatrix}, \tag{2}$$

where with reference to Figure 3, $\mathbf{e}_{si} = L_iN_i/l_i, (i = 1, 2, 3)$ is a unit-vector along the mooring line i, that points from the sea floor anchorage point L_i to the attachment point of the tether N_i; $\mathbf{n}_i$ represents the position of the tether attachment point N_i relative to the buoy centre of mass G, which is also the centre of the system rotation.

The inverse kinematic Jacobian is assessed for the nominal position of the buoy, assuming that the tethers are equally distributed around the buoy and inclined to the vertical at angle α, as shown in Figure 3. This arrangement of mooring lines, when they are separated by 120 degrees in the horizontal plane, provides an independence of surge, sway and heave motions that is beneficial for an axysimmetric WEC, as has been shown in [15]. Moreover, only the equilibrium position case should be considered, as, in reality, a buoy will have motion amplitude constraints, leading to considerably small translational and rotational displacements, compared with the length of the mooring lines. Equation (2) can be expanded as:

$$\mathbf{J}^{-1} = \begin{pmatrix} e_{s1}^x & e_{s1}^y & e_{s1}^z & (n_1^y e_{s1}^z - n_1^z e_{s1}^y) & (n_1^z e_{s1}^x - n_1^x e_{s1}^z) & (n_1^x e_{s1}^y - n_1^y e_{s1}^x) \\ e_{s2}^x & e_{s2}^y & e_{s2}^z & (n_2^y e_{s2}^z - n_2^z e_{s2}^y) & (n_2^z e_{s2}^x - n_2^x e_{s2}^z) & (n_2^x e_{s2}^y - b_2^y e_{s2}^x) \\ e_{s3}^x & e_{s3}^y & e_{s3}^z & (n_3^y e_{s3}^z - n_3^z e_{s3}^y) & (n_3^z e_{s3}^x - n_3^x e_{s3}^z) & (n_3^x e_{s3}^y - n_3^y e_{s3}^x) \end{pmatrix}. \tag{3}$$

Assuming that the water depth is constant for all anchorage points L_i, and the z-components of all vectors $\mathbf{e}_{si}$ are equal to $e_{s1}^z = e_{s2}^z = e_{s3}^z$ and all tether attachment points N_i lie in a horizontal plane parallel to the sea floor, so $n_1^z = n_2^z = n_3^z$. Furthermore, as the mass of the tethers are negligibly small when compared with the mass of the buoy, corresponding vectors $\mathbf{n}_i$ and $\mathbf{s}_i$ will always lie in the same vertical plane, so $e_{s1}^x \sim n_1^x, e_{s2}^x \sim n_2^x, e_{s3}^x \sim n_3^x$ and $e_{s1}^y \sim n_1^y, e_{s2}^y \sim n_2^y, e_{s3}^y \sim n_3^y$ ($\sim$ is used as a linear dependence operator). Thus, it is obvious from Equation (3), that the second and fourth columns of the inverse Jacobian are linearly dependent, likewise the first and fifth ones. This means that there are only three buoy motions that can be independently controlled through three tethers: coupled surge/pitch, coupled sway/roll and heave. As the sixth column of the inverse Jacobian always goes to zero in this configuration, the yaw angle remains uncontrollable, however this is not critical for the axysimmetric bodies because they cannot be excited by waves in yaw in any case.

An inverse Jacobian matrix of parallel mechanisms is conventionally used for the derivation of various dexterity indexes, such as kinematic manipulability [19], or the condition number [22]. In particular the condition number is widely used to determine an optimal design for the robot, considering all the given requirements. For the mechanisms with translational and rotational movement capabilities, the Jacobian matrix that is used to calculate the condition number should be consistent in physical units. One way to derive dimensionally homogeneous inverse Jacobian is to normalise it by dividing its rotational elements by the nominal length of the link [23], so from Equation (2):

$$\bar{\mathbf{J}}^{-1} = \begin{pmatrix} \mathbf{e}_{s1}^\intercal & (\mathbf{n}_1 \times \mathbf{e}_{s1})^\intercal / l_{10} \\ \mathbf{e}_{s2}^\intercal & (\mathbf{n}_2 \times \mathbf{e}_{s2})^\intercal / l_{20} \\ \mathbf{e}_{s3}^\intercal & (\mathbf{n}_3 \times \mathbf{e}_{s3})^\intercal / l_{30} \end{pmatrix}. \tag{4}$$

Assuming that all tethers point towards the centre of the body ($\mathbf{s}_i$ and $\mathbf{n}_i$ are collinear), it is obvious from Equation (4) that the inverse kinematic Jacobian depends only on the inclination angle of tethers included in $\mathbf{e}_{si}$ and $\mathbf{n}_i$, while being independent of water depth and submergence depth of the WEC. The optimal value of this angle can be found using the condition number index, which is calculated as [22]:

$$\kappa(\bar{\mathbf{J}}) = \kappa(\bar{\mathbf{J}}^{-1}) = \left\|\bar{\mathbf{J}}^{-1}\right\| \cdot \left\|\bar{\mathbf{J}}\right\|, \tag{5}$$

where $\|\cdot\|$ defines the two-norm of a matrix, and $\bar{\mathbf{J}}$ can be obtained from Equation (4) using pseudo-inverse. The smallest possible value of the condition number is 1, which relates to the best configuration of mooring lines, where each power take-off system does the same amount of work. Therefore, the objective is to find an inclination angle α which minimises the condition number

$$\min_{\alpha} \kappa(\bar{\mathbf{J}}^{-1}). \tag{6}$$

The condition number given by Equation (5) of the inverse Jacobian has been calculated for the system, varying an inclination angle of three tethers α from 0 (extracting power from the heave only) to 90 degrees (surge/pitch) and the results are shown in Figure 4. In addition, to provide better understanding of the mutual arrangement of the mooring lines, an auxiliary angle (θ) was introduced, that is subtended between two tethers in the plane that they form (θ relates to α as $\cos\theta = 1 - \frac{3}{2}\sin^2\alpha$). Therefore, Figure 4 is supplemented by the upper horizontal scale that demonstrates the related angle between tethers θ. Note that all further figures related to the arrangement of tethers will have two scales for α and θ simultaneously.

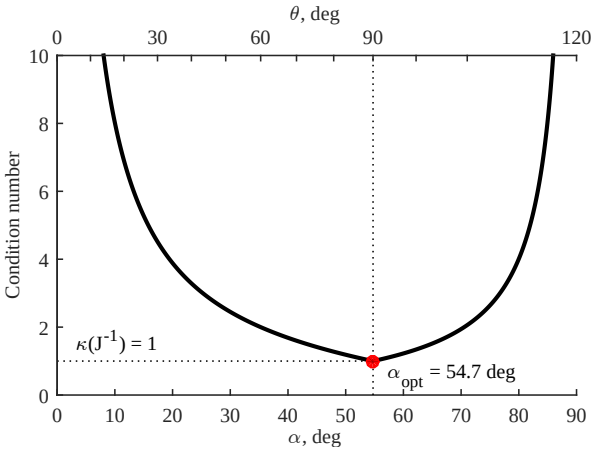

Figure 4: The variation of the condition number with the inclination angle of tethers in the 3-tether configuration. α (lower scale) shows the angle between each tether and the vertical, while θ (upper scale) shows the corresponding angle between the tethers in the plane that they form.

The minimum value of $\kappa(\bar{\mathbf{J}}^{-1})$ is reached at an optimal inclination angle α of 54.7 degrees = $\arccos\left(1/\sqrt{3}\right)$ that corresponds to the orthogonal tethers ($\theta = 90$ degrees) when they form the edges of the cuboidal vertex. Such a configuration, when the condition number κ is equal to 1, is called an isotropic pose [24] indicating that the 3-tether WEC has uniform properties in all directions of motion. As a result, an arrangement of three mooring lines, when they are orthogonal, provides the best translation from the positions and velocities of the buoy to the length and change in length of tethers. Moreover, different locations of tether attachment points to the hull were considered, as well as different aspect ratios of the buoy dimensions to the tether length. It was found that the most optimal arrangement is achieved when all tethers point toward the geometrical centre of the WEC.

3. Dynamic analysis

In this section an optimal arrangement of mooring lines is studied for two generic shapes of WECs: a sphere and a cylinder.

Firstly, the dynamic equations of the WEC are considered, regardless of its shape (the equations have been partially adapted from [10]). With reference to Figure 3, the position of the buoy centre of mass G, relative to the reference coordinate frame $Oxyz$, is denoted by the vector $\mathbf{r}$. In the undisturbed (equilibrium) position, the centre of mass G coincides with the origin O, so $\mathbf{r} = 0$. A vector $\mathbf{s}_i$ is directed along each tether i from the sea floor to the attachment point on the buoy hull. The relative position of the attachment point of the tether to the centre of mass G is denoted by $\mathbf{n}_i$.

Next, the interaction of only one tether with a body is analysed, so the subscript of the tether number $i = 1, 2, 3$ will be eliminated temporarily. As a buoy has positive buoyancy, the tension in each tether is always positive ($T > 0$). The applied force vector of the tether on the buoy is

$$\mathbf{f}_t = -T\mathbf{e}_\mathbf{s}, \tag{7}$$

where $\mathbf{e}_\mathbf{s}$ is a unit vector in the same direction as $\mathbf{s}$.

The vector of angular displacements of the body $\vartheta = (\vartheta_x, \vartheta_y, \vartheta_z)^\intercal$ is taken to be relative to the inertial coordinate frame $Oxyz$, and these angles are zero in the undisturbed position. Considering the 'small angle' approximation, angular rotations are assumed to be independent and a change in the vector $\mathbf{n}$ from $\mathbf{n}_0$ is

$$\delta\mathbf{n} \approx \vartheta \times \mathbf{n}_0 = \mathbf{N}_0\vartheta, \tag{8}$$

where

$$\mathbf{N}_0 = \begin{bmatrix} 0 & n_{0z} & -n_{0y} \\ -n_{0z} & 0 & n_{0x} \\ n_{0y} & -n_{0x} & 0 \end{bmatrix} \tag{9}$$

and a subscript '0' stands for the equilibrium position.

The change in the vector $\mathbf{s}$ from the undisturbed position $\mathbf{s}_0$ is

$$\delta\mathbf{s} = \mathbf{r} + \mathbf{N}_0\vartheta \tag{10}$$

and the linearised change in the tether length is

$$\delta\|\mathbf{s}\| \approx \mathbf{e}_{s0}^\intercal\delta\mathbf{s}, \tag{11}$$

where $\|.\|$ is the Euclidean norm and $\mathbf{e}_{s0}$ is a unit vector in the direction of $\mathbf{s}_0$. The change in the force vector $\mathbf{f}_t$ is

$$\delta\mathbf{f}_t = \delta\left(-\frac{T}{\|\mathbf{s}\|}\mathbf{s}\right) \approx -\mathbf{e}_{s0}\delta t - \frac{T_0}{\|\mathbf{s}_0\|}(\mathbf{I}_3 - \mathbf{e}_{s0}\mathbf{e}_{s0}^\intercal)(\mathbf{r} + \mathbf{N}_0\vartheta). \tag{12}$$

It is assumed that the change in the tether tension is caused by the reaction of the power-take off system, which can be modelled as a linear spring and damper with variables k_t and c_t, such that

$$\delta T = k_t\delta\|\mathbf{s}\| + c_t\frac{d}{dt}\delta\|\mathbf{s}\| = \mathbf{e}_{s0}^\intercal\big(k_t\mathbf{r} + c_t\dot{\mathbf{r}} + \mathbf{N}_0(k_t\vartheta + c_t\dot{\vartheta})\big). \tag{13}$$

Substituting Equation (13) into (12), the change in the tether force can be expressed as:

$$\begin{aligned}\delta\mathbf{f}_t = &-\frac{T_0}{\|\mathbf{s}_0\|}(\mathbf{I}_3 - \mathbf{e}_{s0}\mathbf{e}_{s0}^\intercal)(\mathbf{r} + \mathbf{N}_0\vartheta) \\ &- \mathbf{e}_{s0}\mathbf{e}_{s0}^\intercal\big(k_t\mathbf{r} + c_t\dot{\mathbf{r}} + \mathbf{N}_0(k_t\vartheta + c_t\dot{\vartheta})\big).\end{aligned} \tag{14}$$

The change in the torque $\boldsymbol{\tau}_t$ that acts on the rigid body about its centre of mass due to the tether force is:

$$\delta\boldsymbol{\tau}_t = \delta(\mathbf{n} \times \mathbf{f}_t) \approx \mathbf{n}_0 \times \delta\mathbf{f}_t - \mathbf{f}_{t0} \times \delta\mathbf{n}, \tag{15}$$

where $\mathbf{f}_{t0}$ is a tether force due to the positive buoyancy of the body.

$\mathbf{S}_0$ is defined in a similar way to $\mathbf{N}_0$ and Equations (8) and (14) are substituted in Equation (15), so the change in the torque is calculated as:

$$\delta\boldsymbol{\tau}_t = \frac{T_0}{\|\mathbf{s}_0\|}\mathbf{N}_0(\mathbf{I}_3 - \mathbf{e}_{s0}\mathbf{e}_{s0}^\intercal)(\mathbf{r} + \mathbf{N}_0\vartheta) - \frac{T_0}{\|\mathbf{s}_0\|}\mathbf{S}_0\mathbf{N}_0\vartheta + \mathbf{N}_0\mathbf{e}_{s0}\mathbf{e}_{s0}^\intercal\big(k_t\mathbf{r} + c_t\dot{\mathbf{r}} + \mathbf{N}_0(k_t\vartheta + c_t\dot{\vartheta})\big). \quad (16)$$

So $\delta\mathbf{f}_t$ and $\delta\boldsymbol{\tau}_t$ can be rewritten in a matrix form:

$$\begin{bmatrix}\delta\mathbf{f}_t\\ \delta\boldsymbol{\tau}_t\end{bmatrix} = -\mathbf{K}_t\begin{bmatrix}\mathbf{r}\\ \vartheta\end{bmatrix} - \mathbf{C}_t\begin{bmatrix}\dot{\mathbf{r}}\\ \dot{\vartheta}\end{bmatrix}, \quad (17)$$

when using the fact that $\mathbf{N}_0 = -\mathbf{N}_0^\intercal$,

$$\mathbf{C}_t = c_t\mathbf{G}_t\mathbf{G}_t^\intercal \quad (18)$$

and

$$\mathbf{K}_t = (k_t - \gamma_0)\mathbf{G}_t\mathbf{G}_t^\intercal + \gamma_0\begin{bmatrix}\mathbf{I}_3\\ \mathbf{N}_0^\intercal\end{bmatrix}\begin{bmatrix}\mathbf{I}_3 & \mathbf{N}_0\end{bmatrix} + \begin{bmatrix}\mathbf{0}_{3\times3} & \mathbf{0}_{3\times3}\\ \mathbf{0}_{3\times3} & \gamma_0\mathbf{S}_0\mathbf{N}_0\end{bmatrix}, \quad (19)$$

where $\mathbf{G}_t = -\begin{bmatrix}\mathbf{I}_3\\ \mathbf{N}_0^\intercal\end{bmatrix}\mathbf{e}_{s0}$ and $\gamma_0 = T_0/\|\mathbf{s}_0\|$.

In the case when all tethers point toward the centre of mass of the buoy, as shown in Figure 5, $\mathbf{n}_0$ and $\mathbf{s}_0$ become collinear and it can be shown that $\mathbf{N}_0\mathbf{e}_{s0}\mathbf{e}_{s0}^\intercal = \mathbf{e}_{s0}\mathbf{e}_{s0}^\intercal\mathbf{N}_0 = \mathbf{0}_{3\times3}$. Therefore, $\mathbf{K}_t$ and $\mathbf{C}_t$ are:

$$\mathbf{K}_t = \begin{bmatrix}(k_t - \gamma_0)\mathbf{e}_{s0}\mathbf{e}_{s0}^\intercal + \gamma_0\mathbf{I}_3 & \gamma_0\mathbf{N}_0\\ \gamma_0\mathbf{N}_0^\intercal & \gamma_0(\mathbf{N}_0^\intercal\mathbf{N}_0 + \mathbf{S}_0\mathbf{N}_0)\end{bmatrix}, \quad (20)$$

$$\mathbf{C}_t = \begin{bmatrix}\mathbf{e}_{s0}\mathbf{e}_{s0}^\intercal c_t & \mathbf{0}_{3\times3}\\ \mathbf{0}_{3\times3} & \mathbf{0}_{3\times3}\end{bmatrix}. \quad (21)$$

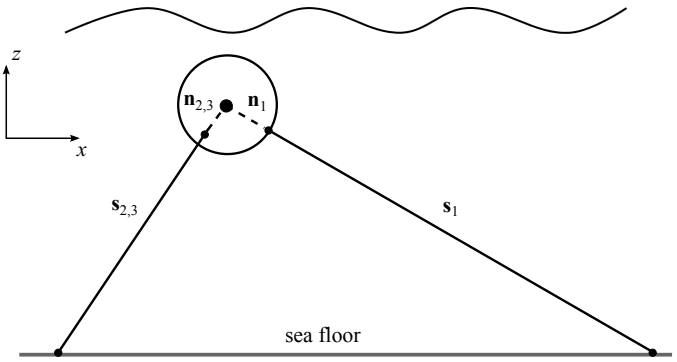

Figure 5: The mooring configuration when all three tethers point toward the centre of mass of the buoy (plane view).

Expanding to the case with three tethers, the total generalised force that acts on the body through the PTO system is:

$$\mathbf{F}_{pto} = \begin{bmatrix}\delta\mathbf{f}_{t1} + \delta\mathbf{f}_{t2} + \delta\mathbf{f}_{t3}\\ \delta\boldsymbol{\tau}_{t1} + \delta\boldsymbol{\tau}_{t2} + \delta\boldsymbol{\tau}_{t3}\end{bmatrix} = -\tilde{\mathbf{K}}_t\mathbf{x} - \tilde{\mathbf{C}}_t\dot{\mathbf{x}}, \quad (22)$$

where $\tilde{\mathbf{K}}_t = \sum_{i=1}^3 \mathbf{K}_{ti}$ and $\tilde{\mathbf{C}}_t = \sum_{i=1}^3 \mathbf{C}_{ti}$, $\mathbf{x} = [\mathbf{r} \quad \vartheta]^\intercal$.

The dynamic equation of the submerged buoy motion is [7]:

$$\mathbf{M}\ddot{\mathbf{x}} = \mathbf{F}_{exc} + \mathbf{F}_{rad} + \mathbf{F}_{pto}, \quad (23)$$

where $\mathbf{M}$ is a mass matrix of the buoy, $\mathbf{F}_{exc}$ is the excitation force vector due to the incident wave, $\mathbf{F}_{rad}$ is the hydrodynamic radiation force vector due to the added mass and damping.

Additional forces acting on the WEC, such as mooring line forces, viscous drag and static drift forces, are not considered in the present analysis. The viscous and inertial mooring line forces are neglected in the model as they are significantly smaller than the wave excitation force for relatively small displacements at typical frequencies [13, 25]. In case when mooring lines are just used to keep body on site and are not involved in power generation, a stiffness of the mooring system can significantly affect the dynamic behaviour of the buoy [26], especially motion in surge. For this kind of problems, an additional tension from the catenary cable or tether is expressed in terms of the supplementary mooring stiffness matrix [27]. However, for the current WEC, where all tethers are connected to individual PTO systems, the behaviour of the mooring system is driven by the PTO stiffness and damping. This is similar to the mechanism of two springs connected in series, where stiffness of the mooring lines is several orders of magnitude higher than that of the PTO system. Thus, considering values used in [26] for the low rotation steel rope, the tether stiffness is around 5.6 MN/m, while a range of the required PTO stiffness should be $\approx 0.1 \ldots 1$ MN/m for a similar WEC size, which supports the assumption made earlier. In case of the static drift force, similar to the net buoyancy force, it can be overcome by initial tension in tethers T_0. Thus, pretension in each tether will be different depending on the wave direction. As a linearised model in Equation (23) allows to incorporate only waves of small amplitudes, the corresponding drift force has a negligible effect on the body dynamics. In contrast, when considering larger waves in the time domain, inclusion of the mean drift force may be necessary.

Fourier transforms of all forces and dynamic states of the buoy are introduced as $\mathcal{F}(\mathbf{r}) = \hat{\mathbf{r}}(j\omega)$; therefore, the hydrodynamic radiation force in the frequency domain can be expressed as:

$$\hat{\mathbf{F}}_{rad} = -\left(j\omega\mathbf{A}(\omega) + \mathbf{B}(\omega)\right)\hat{\dot{\mathbf{x}}}, \quad (24)$$

where $\mathbf{A}(\omega)$ is a hydrodynamic added mass matrix and

$\mathbf{B}(\omega)$ is a matrix of damping coefficients. The PTO force in the frequency domain can be expressed as:

$$\hat{\mathbf{F}}_{pto} = -\left(j\frac{\tilde{\mathbf{K}}_t}{\omega} - \tilde{\mathbf{C}}_t\right)\hat{\dot{\mathbf{x}}}, \tag{25}$$

and the dynamic equation (23) can be rewritten as:

$$\left(\mathbf{Z}_{pto}(\omega) + \mathbf{Z}_{buoy}(\omega)\right)\hat{\dot{\mathbf{x}}} = \hat{\mathbf{F}}_{exc}, \tag{26}$$

where the hydrodynamic impedance of the submerged body is $\mathbf{Z}_{buoy}(\omega) = \mathbf{B}(\omega) + j\omega(\mathbf{M} + \mathbf{A}(\omega))$ and the impedance of the PTO system is $\mathbf{Z}_{pto}(\omega) = \tilde{\mathbf{C}}_t - j\frac{\tilde{\mathbf{K}}_t}{\omega}$.

Let us denote the complex velocity amplitude as $\hat{\mathbf{u}} = \hat{\dot{\mathbf{x}}}$. The averaged power absorbed by the system is [28]:

$$P(\hat{\mathbf{u}}) = \frac{1}{4}(\hat{\mathbf{F}}^*_{exc}\hat{\mathbf{u}} + \hat{\mathbf{u}}^*\hat{\mathbf{F}}_{exc}) - \frac{1}{2}\hat{\mathbf{u}}^*\mathbf{B}\hat{\mathbf{u}}, \tag{27}$$

where * denotes the conjugate transpose.

The maximum power can be absorbed when the velocity of the system is unconstrained and equal to $\hat{\mathbf{u}}_0 = \frac{1}{2}\mathbf{B}^{-1}\hat{\mathbf{F}}_{exc}$ [7]. However, in reality the velocity value is limited due to the capacity of the components. For example, the stroke of the PTO hydraulic piston limits the maximum displacement of the buoy, which in turn determines the maximum velocity of the WEC as $\hat{\mathbf{u}} \leq \hat{\mathbf{u}}_{\max} = \omega\hat{\mathbf{x}}_{\max}$. In addition, the velocity of the system is not only a function of k_t and c_t control parameters, but also depends on the tether inclination angle α. Therefore, the following optimisation procedure is performed to find an optimal arrangement of the mooring lines:

(i) calculate the hydrodynamic parameters of the WEC $(\mathbf{A}(\omega), \mathbf{B}(\omega), \hat{\mathbf{F}}_{exc}(\omega))$ for a particular buoy configuration (e.g. shape, submergence depth, ocean depth);

(ii) express the complex velocity $\hat{\mathbf{u}}$ as a function of k_t, c_t and α

$$\hat{\mathbf{u}}(k_t, c_t, \alpha) = \left(\mathbf{Z}_{pto} + \mathbf{Z}_{buoy}\right)^{-1}\hat{\mathbf{F}}_{exc}; \tag{28}$$

(iii) maximise the average power of the system using Equation (27), so

$$\max_{\alpha, k_t, c_t} P(\hat{\mathbf{u}}) \quad \text{subject to } \hat{\mathbf{u}} \leq \hat{\mathbf{u}}_{\max}. \tag{29}$$

A rigid body has different resonant frequencies in each uncoupled mode of oscillation. For example, the natural frequency of the surging WEC approaches zero [29], while the natural period for heave resonance is short compared with the dominant wave periods [30]. Therefore, the physical meaning of this optimisation procedure is to find such a configuration of mooring lines where the resonant frequencies of heave and surge/pitch motion modes coincide, leading to maximum power absorption.

Two distinct shapes will be considered for optimisation purposes: a sphere and a vertical cylinder. There are several reasons to explain the choice of two bodies. First of all, a cylinder represents a simple classical example of the axisymmetric body that can be excited by ocean waves in heave, surge and pitch modes, meanwhile, a sphere has a unique feature in not being able to radiate waves from any angular motion. Furthermore, the hydrodynamic models of these two bodies can be found analytically and are studied extensively in the literature.

Due to the fact that WECs may have different design properties and operate under diverse sea site conditions, the effect of various parameters on the optimal solution is covered in Sections 3.1–3.6. All sensitivity studies are performed for the spherical body except Section 3.5, where vertical cylinders with different aspect ratios are taken into consideration. It should be noted, that all trends presented for the spherical body are applicable for the cylinder. All results in the following sections have been found limiting displacements of the WEC in heave and surge to $0.5a$ and taking a regular wave amplitude as $A = 0.2a$. Parameters used in the following analysis are listed in Table 1, where the sensitivity study is based on the column 'Range for sensitivity analysis' while other WEC parameters are set according to the 'Fixed value' column. 'Body shape' shows what WEC device is used in the corresponding section.

3.1. Sensitivity to the submergence depth

The hydrodynamic (radiation and diffraction) parameters of the spherical body in finite depth are obtained using the analytical model presented in [31]. This model utilises the multi-pole expansion method with the linear wave theory approximation, where the fluid is assumed to be inviscid, incompressible and irrotational [7]. Due to its symmetrical shape, the sphere is excited by ocean waves in heave and surge modes that are hydrodynamically uncoupled.

The optimisation procedure according to Equation (29) is obtained using the MATLAB Optimization Toolbox. Figure 6 demonstrates the dependence of the optimal inclination angle on the non-dimensional wavenumber ka for various submergence depths of the sphere $d_s = 1.25a$, $1.5a$, $1.75a$, $2a$ and $3a$. The ocean depth is taken as $h = 10a$. The range of ka is chosen on the basis of existing WEC prototypes (e.g. Carnegie CETO system). Thus, ka takes values between 0.1 and 2, which covers the region of wave periods from 5 to 18 sec with a radius of the device $a =$ 10 m ($1.61 > ka = a\omega^2/g > 0.12$). As the sphere should be positively buoyant, the value of the mass is chosen as $m_b/m_w = 0.85$, where m_w is the mass of water displaced by the buoy.

As shown in Figure 6, all curves lie around an optimal inclination angle of 54.7 degrees within a range of ± 1.5 degrees. These results are in a good agreement with the kinematic analysis performed in Section 2. Moreover, the deeper the body is submerged, the less sensitive is the optimal angle to the wave frequency.

3.2. Sensitivity to the water depth

The range of water depth in the current analysis is chosen to represent shallow, intermediate and deep wa-

Table 1: WEC parameters used in optimisation and sensitivity studies.

Parameter	Notation	Body shape	Fixed value	Range for sensitivity analysis
Submergence depth	d_s/a	sphere	1.75	1.25, 1.5, 1.75, 2, 3
Water depth	h/a	sphere	10	5, 6, 7, 8, 9, 10
Mass ratio	m_b/m_w	sphere	0.85	0.15, 0.3, 0.5, 0.7, 0.85
Wave direction		sphere	0 deg	-30, -20, -10, 0, +10, +20, +30 deg
Body height	H/a	cylinder		0.5, 1, 1.5, 2, 2.5, 3
Number of control parameters		sphere	3	3, 4, 5
Wave height	A/a		0.2	
Motion constraint			$0.5a$	

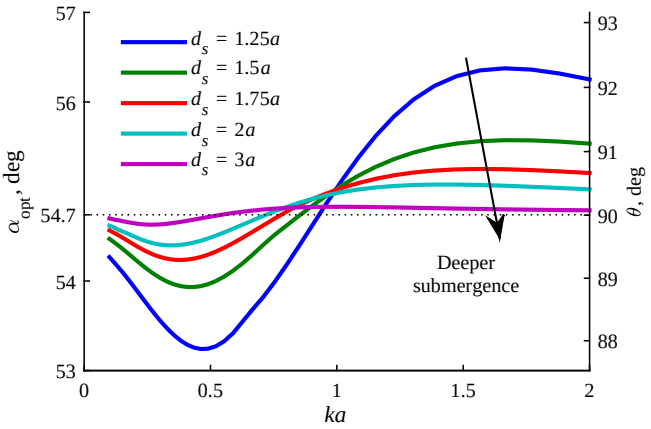

Figure 6: The optimal inclination angle of mooring lines of the sphere vs. non-dimensional wavenumber ka for different submergence depth d_s, water depth is $h = 10a$.

ter, such as $h = 5a$, $6a$, $7a$, $8a$, $9a$ and $10a$ (Figure 7). The lowest value of $h = 5a$ is dictated by limitations of a linearised frequency-domain model, while the maximum value of $h = 10a$ is chosen to represent deep water because hydrodynamic coefficients of the sphere at $h = 10a$ are very close to the infinite water depth results [31].

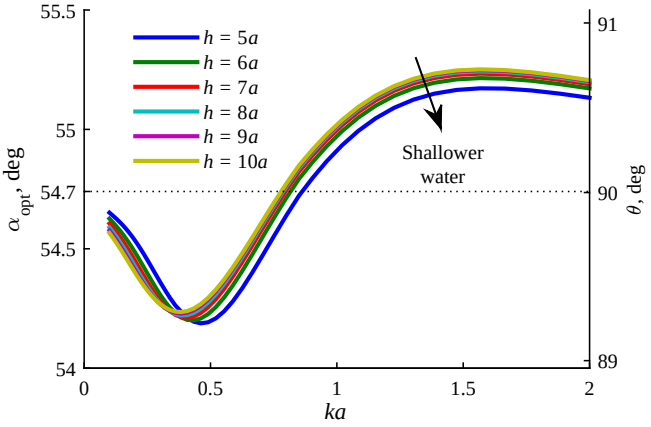

Figure 7: The optimal inclination angle of mooring lines of the sphere vs. non-dimensional wavenumber ka for different water depth h, submergence depth is $d_s = 1.75a$.

As shown in Figure 7, the ocean depth has a negligible affect on the values of the optimal inclination angle, even though shallower water increases the excitation force in surge and decreases the force in heave. The maximum difference between angles for the shallow and deep water is less than 0.2 degrees over the range of wave frequencies.

3.3. Sensitivity to the mass of the buoy

Mass plays an important role in the WEC design as it determines the net buoyancy force and initial tension in all tethers. Also when a buoy is connected to the sea floor through flexible tethers (not rigid rods), they may become slack if the required PTO force is larger than the pretension force. Therefore, the device should be light enough to guarantee taut tethers all the time.

The range of masses for the analysis is chosen from similar prototypes [10, 15] and covers values from 0.15 to $0.85m_w$. Figure 8 shows that the heavier buoy is, the less sensitive is the optimal angle to the wave frequency.

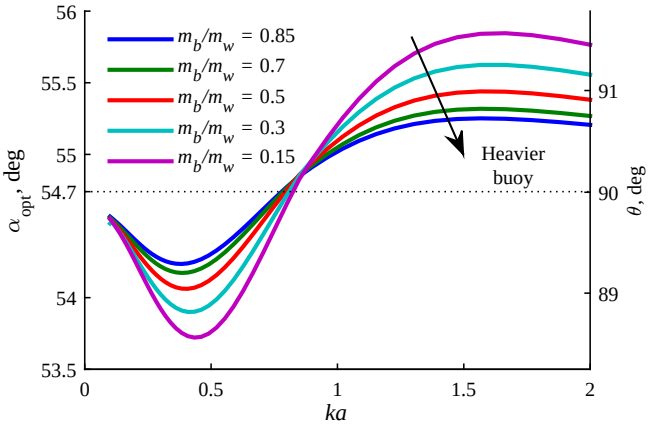

Figure 8: The optimal inclination angle of mooring lines of the sphere vs. non-dimensional wavenumber ka for different ratios of the buoy mass to mass of displaced water m_b/m_w.

The occurrence of tether slackness is directly dependent on the wave amplitude and frequency. Thus, the optimally controlled buoy with a mass of $m_b/m_w = 0.85$ at regular waves of 1 m amplitude will experience slackness of tethers at frequencies $ka > 0.16$, almost every cycle of

motion. This reduces the total power absorption of the WEC, as power take-off system is not able to extract energy when a tether is slack. In contrast, for $m_b/m_w = 0.5$ tethers become loose only at $ka > 1.2$, which is more suitable for power conversion purposes.

In addition, the buoy mass (through the net buoyancy force and moment of inertia) determines the resonance frequency of the WEC in pitch and roll. It can be seen from Equation (20) that the frequency response of surge, sway and heave modes can be changed using a spring control parameter k_t. In contrast, the natural frequencies of angular modes are predominantly dependent on the initial tension and length of tethers through γ_0-parameter and cannot be directly controlled. Thus, for the spherical buoy with a mass ratio of $m_b/m_w = 0.85$, which is submerged to $d_s = 1.75a$ at water depth of $h = 10a$, the natural frequency of pitch mode occurs around $ka = 0.3$. This is within the range of operational sea sites frequencies, which is not desirable for the current WEC design. A reduction in mass leads to an increase in the pitch natural frequency, and can be used to move the pitch response outside the frequency range of interest.

3.4. Sensitivity to the wave direction

The direction of wave propagation may vary greatly depending on the sea site. Consequently an optimisation has been performed for the range of wave angles from -30 to 30 degrees with a 10-degree increment, which covers all possible wave direction options due the cyclic axisymmetry of the tripod configuration. In the investigation it was found that wave direction does not affect the optimal parameters of the PTO and a tether inclination angle have the same dependence on the frequency for all incident wave angles. The only difference in the WEC performance is that the distribution of power absorption between three tethers varies depending on the wave direction.

3.5. Sensitivity to aspect ratio of the body

A spherical body has an aspect ratio of 1 as its vertical and horizontal dimensions are equal. In case of a cylinder, the aspect ratio may be different varying from a flat, disk-shaped body to the infinitely long cylinder. The dimensions of a WEC determine the ratio between horizontal and vertical excitation forces that act on the body. This in turn affects the distribution of power absorption between heave and surge motion modes, that will influence the optimal inclination angle of the three-tether mooring system.

An analytical model of all hydrodynamic parameters of a submerged vertical cylinder in finite depth is obtained from [32, 33]. Unlike the spherical case, the cylinder is excited in surge, heave and pitch modes with a coupling in surge/pitch. It means that the added mass matrix $\mathbf{A}(\omega)$ and the matrix of damping coefficients $\mathbf{B}(\omega)$ have off-diagonal elements.

Figure 9 demonstrates the comparison of the optimal configuration of tethers for the equally submerged ($d_s = 2a$) vertical cylinders with various aspect ratios ($H = 0.5a, 1a, 1.5a, 2a, 2.5a$ and $3a$). For the cylinder with an aspect ratio of one ($H = 2a$), the curve lies around an optimal inclination angle of 54.7 degrees (orthogonal tethers), but with a greater variation around an optimal point compared with the spherical case. For other cylinder geometries the tether arrangement is highly dependent on the body aspect ratio.

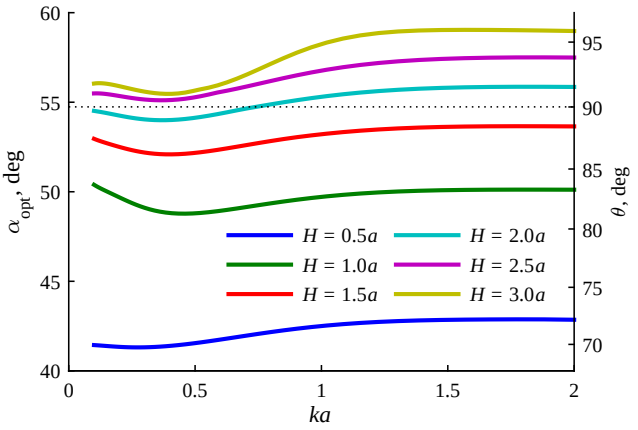

Figure 9: A comparison of an optimal inclination angle of mooring lines for vertical cylinders with different aspect ratios ($H = 0.5a, a, 1.5a, 2a, 2.5a, 3a$). All bodies are submerged to the same depth of $d_s = 2a$, the ocean depth is $h = 10a$, mass of cylinders is $m_b/m_w = 0.85$.

It is apparent from Figure 9, that flat cylinders ($H < 2a$) require the tether angle to be smaller than the optimal 54.7 degrees as they rely more on heave, thus the mooring lines are closer to the vertical. This is opposed to the slender cylinders ($H > 2a$), where the surge mode is dominant and tethers should have a larger inclination angle.

3.6. Sensitivity to the number of control parameters

Results in Sections 3.1–3.5 are obtained assuming that all three power take-off systems have identical values of control stiffness and damping coefficients ($k_{t1,2,3} = k_t$, $c_{t1,2,3} = c_t$). This makes the WEC insensitive to the direction of wave propagation, where optimal control parameters can be detected for different sea states and then applied regardless of the incoming wave angle.

To investigate the effect of the number of control parameters on the optimal tether configuration, a spherical WEC is considered. Taking into account that the system is symmetric about xz-coordinate plane, tethers 2 and 3 will require identical PTO settings if wave propagates along the x-axis. Thus, four different combinations of independent control parameters are introduced:

'3' – all tethers have identical values of stiffness and damping coefficients ($k_{t1,2,3} = k_t$, $c_{t1,2,3} = c_t$), therefore three unknowns, such as α, k_t, c_t are included in the optimisation;

'4k' – all tethers have individual values of spring stiffness while damping coefficients will remain the same for all PTOs. Therefore, the optimisation procedure will include four unknowns, such as $\alpha, k_{t1}, k_{t2,3}, c_t$;

'4c' – all tethers have individual damping while stiffness coefficients will remain the same for all PTOs resulting in four unknowns, such as $\alpha, k_t, c_{t1}, c_{t2,3}$;

'5' – all tethers have individual control parameters leading to five optimisation parameters $\alpha, k_{t1}, k_{t2,3}, c_{t1}, c_{t2,3}$.

As a result, the objective function in Equation (29) is modified according to the above four cases. Hereinafter, each of the proposed combinations will be referred to as '3', '4k', '4c' and '5'-system.

Figure 10 shows a variation in the optimisation results between systems for the test case of a fully submerged spherical body (submergence depth is $d_s = 1.75a$, water depth is $h = 10a$, wave amplitude is $A = 0.2a$, motion is constrained to $0.5a$ in heave and surge, mass of the buoy is $m_b/m_w = 0.85$).

From Figure 10b it can be seen, that '3'-system absorbs slightly less than the maximum power, while '4k', '4c' and '5' cases approach the theoretical maximum. Also, there is no need to use independent parameters for all tethers (as in case '5') since '4k' and '4c'-systems can provide the maximum power output (lines on the plot overlap). The data for the inclination angle of the 5-parameter system (Figure 10a) is not smooth indicating that a system is poorly conditioned (overdetermined) and there are many combinations of PTO parameters which achieve maximum power absorption. Since the spring and damper coefficients for this system have the same 'noisy' behaviour, they are not displayed on Figures 10c and 10d.

The main difference in results is associated with the damping coefficient (c_t) shown on Figure 10d. It is interesting to note that in case of '4c' optimisation, the values of the damping coefficient for tethers 2 and 3 are several times larger than that for the tether 1; whereas the spring coefficients differ slightly for all optimisation procedures (Figure 10c). Also, systems with '3' and '4k' parameters are very close in terms of the optimal angle, while a curve for the 5-parameter system oscillates around those values. The WEC with the independent damping control over each tether requires a larger angle between mooring lines as compared to other systems.

However, despite these obvious discrepancies in results, the normalised power absorption of the system with identical control parameters for each tether is only 2.7% less than for the WEC with individual control over all PTOs. Nonetheless, due to the uneven distribution of damping or stiffness coefficients over all tethers, tether 1 for the 4- and 5-parameter systems experiences 10.8% higher load as compared to the 3-parameter counterpart. This is undesirable from an engineering perspective since it increases the capital cost of the system considerably for only a marginal increase in power production. Another issue associated with independent control parameters is that the optimal damping of the first tether is found to be 0 for the '4c' case. This means that the first PTO system will not absorb any power at frequencies $ka > 0.6$.

Therefore, the use of individual control parameters for all PTO systems does not have a huge impact on the optimal inclination angle of tethers, but may improve the relative capture width (RCW) of the WEC. Such a rise in power absorption is accompanied by a significant increase in the load on tether 1, which may be critical for the WEC design. A corresponding compromise between power and tension force makes it necessary to conduct a techno-economic analysis in order to assess systems with different sets of control parameters, which goes beyond the scope of this article.

Moreover, it should be pointed out that individual tuning of all PTO systems introduces additional complexity of the control system design. Since the improvement in the WEC performance is very minor with respect to the difficulty of the problem; the same control parameters have been considered in Sections 3.1–3.5.

4. Effect of the tether configuration on power absorption

Sections 2 and 3 demonstrated how the optimal angle of tethers is sensitive to various parameters, such as a submergence depth of the buoy or its mass. However, the most important question is how this angle affects the total power absorption of the WEC assuming optimal settings of the PTO system, since it is not always possible to achieve the optimal configuration of tethers in practice, e.g. due to geological features of the sea site.

Depending on the parameters that define the system, optimal values of the inclination angle may be almost insensitive to the wave frequency or may vary greatly across the entire frequency range. Therefore, WECs that represent these two cases will be chosen for the analysis: case 1 shows a sensitive system, where a WEC is located close to the water level with a low mass ratio, and case 2 relates to the insensitive system (a heavy buoy that is deeply submerged).

Figure 11 demonstrates the influence of the inclination angle of tethers on the power output (relative capture width) for these two cases. The solid lines correspond to the optimal solution that maximises the relative capture width, while shaded areas show the range of inclination angles in which RCW falls within 99% of its maximum value. Thus, for the first case, where the optimal angle is quite sensitive to the wave frequency, the deviation from the optimum in few degrees has a minor impact on the power absorption. Interestingly, the trend is opposite for the second case, where the optimal solution is almost insensitive to the wave frequency, but the power output is highly dependant on the inclination angle. To give more insight to the second case, the corresponding RCW for various inclination angles of tethers $\alpha = 50 \dots 60$ degrees is

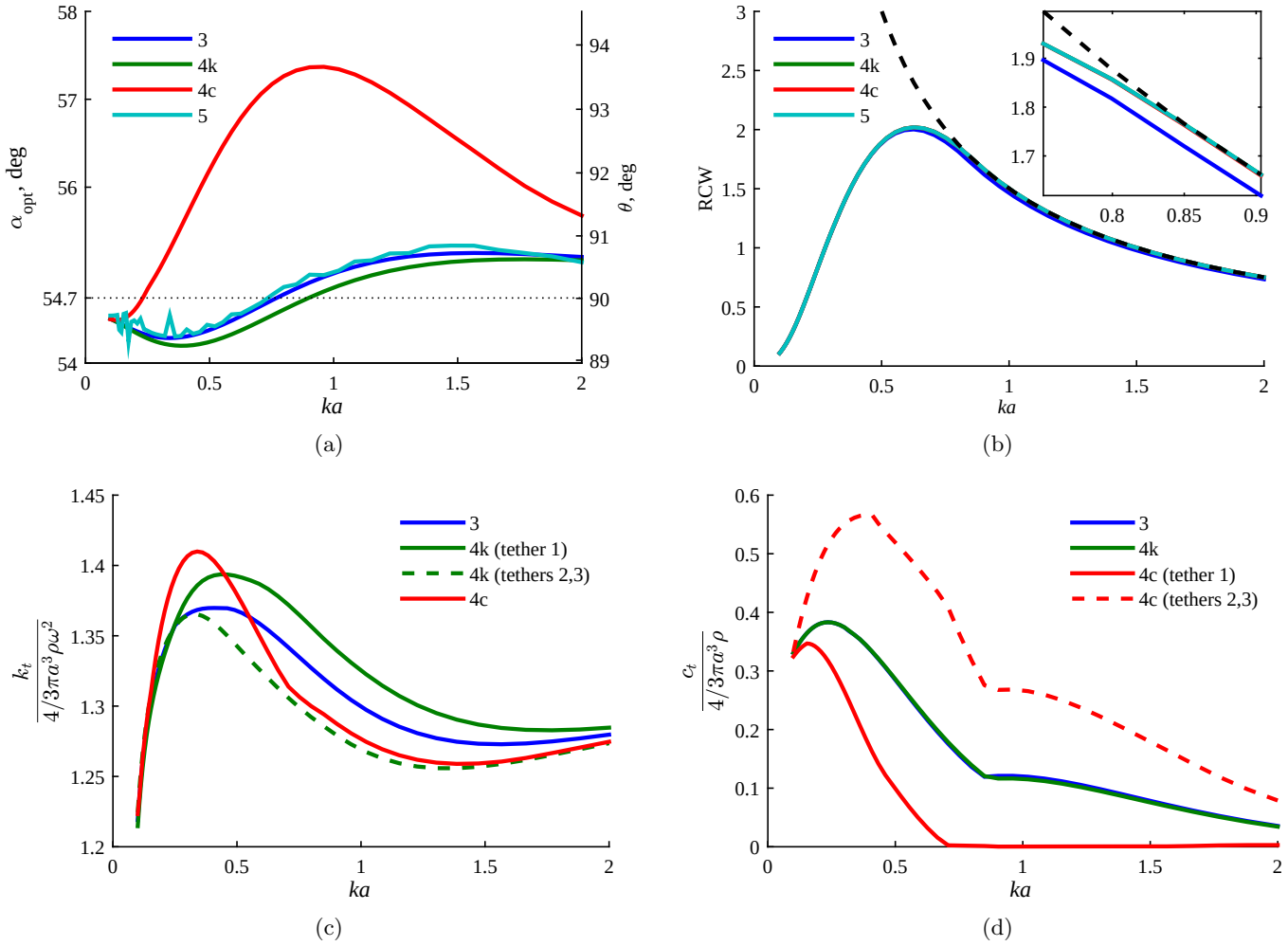

Figure 10: Comparison in results for four optimisation procedures (the black dashed line corresponds to the theoretical maximum): (a) inclination angle of tethers; (b) relative capture width; (c) non-dimensional PTO stiffness; (d) non-dimensional PTO damping.

depicted on Figure 12. Thus, for long waves ($ka < 0.5$), a change in the angle by 1-2 degrees causes the reduction of power absorption by no more than 1%, while for short waves ($ka > 1$) even small variations from the optimal solution can involve a sudden drop in the WEC efficiency. However, as the majority of devices target long waves, an inaccuracy of several degrees in the mooring lines installation is acceptable for the three-tether WEC.

In summary, whilst for low frequencies a small error in the tether angle has a negligible effect on the power output of the system, at high frequencies this is no longer the case. Therefore, in some cases it may be necessary to select the arrangement of the tethers such that the system targets a particular sea site.

5. Discussion

Despite the fact that the current study is based on frequency domain analysis utilising linear wave theory and idealised power take-off systems, it should be used as a reference for further investigation of the optimal mooring configurations, taking into account site-specific features, such as typical spectra of the sea state and WEC design limitations. Moreover, non-linear effects such as viscous losses and non-linear dynamics of the hydraulic power take-off system may influence the results presented in this article. At the same time, the three-tether mooring configuration where all tethers are perpendicular to each other (forming the edges of a cuboidal vertex) and point towards the centre of mass of the buoy should be used as a starting point for further design optimisation and control system development. Current analysis will be extended to irregular wave conditions using a time-domain model in order to validate the main findings of this paper. Also future work involves validation of the concept using a scale-model experiment.

6. Conclusions

An optimal arrangement of the 3-tether mooring configuration has been investigated for two generic shapes of

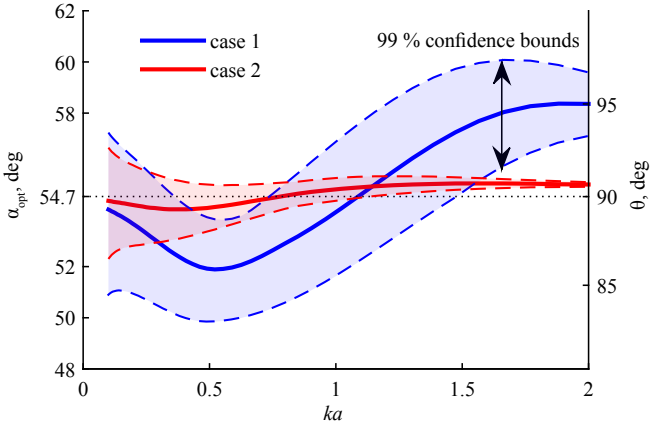

Figure 11: The influence of the tether inclination angle on the relative capture width of the system. Case 1 (blue) corresponds to a system where the optimal solution of the tether inclination angle is very sensitive to the wave frequency (a sphere with $d_s = 1.25a$ and $m_b/m_w = 0.15$); while case 2 (red) corresponds to a system, where the optimal tether angle is almost insensitive to the wave frequency (a sphere with $d_s = 1.75a$ and $m_b/m_w = 0.85$). Solid lines show the optimum values that maximise the output power, while broken lines limit the area where RCW falls within 99% of it maximum value.

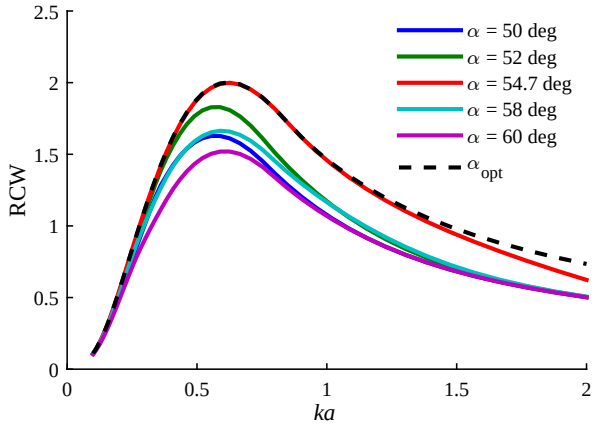

Figure 12: The sensitivity of the relative capture width to a variation of the tether inclination angle (corresponds to the case 2 from Figure 11). A black broken line shows RCW when the inclination angle is optimal for each frequency.

submerged point-absorbing WECs in frequency domain using a linear wave theory approximation and a linear power take-off system. Since such a configuration allows the extraction of power from surge, heave and pitch motions, the relative contribution from each mode in the absorption of power is different and depends on the inclination angle of mooring lines. Assuming that all tethers are equally distributed around a buoy (120 degrees between tethers in a horizontal plane), the objective of this study is to optimise the inclination angle of tethers in order to reach maximum power absorption. The kinematic study of the problem has shown that all tethers should be orthogonal to each other, allowing all power take-off systems to do the same amount of work. This arrangement turned out to be optimal also for the submerged spherical WEC and for the submerged vertical cylinder with an aspect ratio of one. The analysis of the cylinders with other aspect ratios revealed that more slender cylinders require a larger inclination angle of tethers to the vertical. This can be explained by the fact that the excitation force in surge increases with the height of the cylinder and therefore more energy can be extracted from the surge oscillation if the same motion constraints are applied. Since the optimal inclination angle of tethers to the vertical for the heaving device is 0 degrees (vertical) and for the surging device is 90 degrees (horizontal), the increase in the height of the cylinder implies a larger inclination angle. It should be noted that with the change of the submergence depth, the dependence of the optimal angle on the incoming wave frequency decreases. In addition, it has been revealed that WECs that have an individual control laws for each tether may require slightly different inclination of mooring lines for optimal power absorption. The minor gains in power absorption come at a cost of increased dynamic loads on the PTOs and added complexity.

Acknowledgements

The authors would like to thank Prof. M. A. Srokosz and Prof. I. V. Sturova for their assistance with the modelling.

References

[1] J. Hayward, P. Osman, The potential of wave energy, Report, CSIRO (2011).

[2] B. Drew, A. R. Plummer, M. N. Sahinkaya, A review of wave energy converter technology, Proceedings of the Institution of Mechanical Engineers, Part A: Journal of Power and Energy 223 (8) (2009) 887–902. doi:10.1243/09576509jpe782.

[3] J. Cruz, Ocean wave energy: current status and future prespectives, Green Energy and Technology, Springer Berlin Heidelberg, Berlin, 2008. doi:10.1007/978-3-540-74895-3.

[4] K. Budar, J. Falnes, A resonant point absorber of ocean-wave power, Nature 256 (5517) (1975) 478–479. doi:10.1038/256478a0.

[5] D. V. Evans, A theory for wave-power absorption by oscillating bodies, Journal of Fluid Mechanics 77 (1) (1976) 1–25. doi:10.1017/S0022112076001109.

[6] J. N. Newman, Marine hydrodynamics, MIT press, 1977.

[7] J. Falnes, Ocean waves and oscillating systems: Linear interactions including wave-energy extraction, Cambridge University Press, 2002.

[8] G. Hagerman, Wave energy systems for recharging AUV energy supplies, in: Proceedings of the 2002 Workshop on Autonomous Underwater Vehicles, 2002, pp. 75–84. doi:10.1109/AUV.2002.1177207.

[9] A. Babarit, A. Clement, J. Ruer, C. Tartivel, Searev: A fully integrated wave energy converter, in: Proceedings of the OWEMES09, 2006. doi:10.1016/j.apor.2006.05.002.

[10] J. T. Scruggs, S. M. Lattanzio, A. A. Taflanidis, I. L. Cassidy, Optimal causal control of a wave energy converter in a random sea, Applied Ocean Research 42 (2013) (2013) 1–15. doi:10.1016/j.apor.2013.03.004.

[11] S. H. Salter, World progress in wave energy – 1988, International journal of ambient energy 10 (1) (1989) 3–24. doi:10.1080/01430750.1989.9675119.

[12] J. Fitzgerald, L. Bergdahl, Including moorings in the assessment of a generic offshore wave energy converter: A frequency domain approach, Marine Structures 21 (1) (2008) 23–46. doi:10.1016/j.marstruc.2007.09.004.

[13] E. E. Bachynski, Y. L. Young, R. W. Yeung, Analysis and optimization of a tethered wave energy converter in irregular waves, Renewable Energy 48 (2012) 133–145. doi:10.1016/j.renene.2012.04.044.

[14] M. J. Muliawan, Z. Gao, T. Moan, A. Babarit, Analysis of a two-body floating wave energy converter with particular focus on the effects of power take-off and mooring systems on energy capture, Journal of Offshore Mechanics and Arctic Engineering 135 (3) (2013) 031902. doi:10.1115/OMAE2011-49135.

[15] M. A. Srokosz, The submerged sphere as an absorber of wave power, Journal of Fluid Mechanics 95 (4) (1979) 717–741. doi:10.1017/S002211207900166X.

[16] S. M. Lattanzio, J. T. Scruggs, Maximum power generation of a wave energy converter in a stochastic environment, in: 2011 IEEE International Conference on Control Applications (CCA), pp. 1125–1130. doi:10.1109/CCA.2011.6044428.

[17] Carnegie Wave Energy Limited, What is CETO?, accessed 15 January 2015.
URL http://www.carnegiewave.com/ceto-technology/what-is-ceto.html

[18] A. Babarit, J. Hals, M. Muliawan, A. Kurniawan, T. Moan, J. Krokstad, Numerical estimation of energy delivery from a selection of wave energy converters – final report, Report, Ecole Centrale de Nantes & Norges Teknisk-Naturvitenskapelige Universitet (2011).

[19] T. Yoshikawa, Manipulability of robotic mechanisms, The international Journal of Robotics Research 4 (2) (1985) 3–9. doi:10.1177/027836498500400201.

[20] P. Choudhury, A. Ghosal, Singularity and controllability analysis of parallel manipulators and closed-loop mechanisms, Mechanism and Machine Theory 35 (10) (2000) 1455–1479. doi:10.1016/S0094-114X(00)00003-3.

[21] S. Mekid, Introduction to parallel kinematic machines, The CRC Press Series in Mechanical and Aerospace Engineering, CRC Press, 2008, pp. 193–220. doi:10.1201/b15822-610.1201/b15822-6.

[22] J.-P. Merlet, Jacobian, manipulability, condition number, and accuracy of parallel robots, Journal of Mechanical Design 128 (1) (2006) 199–206. doi:10.1115/1.2121740.

[23] S.-G. Kim, J. Ryu, New dimensionally homogeneous jacobian matrix formulation by three end-effector points for optimal design of parallel manipulators, Robotics and Automation, IEEE Transactions on 19 (4) (2003) 731–736.

[24] J.-P. Merlet, Jacobian, manipulability, condition number and accuracy of parallel robots, Springer, 2007, pp. 175–184. doi:10.1007/978-3-540-48113-3_16.

[25] E. E. Bachynski, Y. L. Young, R. W. Yeung, Analysis and dynamic scaling of tethered wave energy converters in irregular waves, in: Proceedings of the International Conference on Offshore Mechanics and Arctic Engineering, Vol. 5, pp. 563–572. doi:10.1115/OMAE2011-49684.

[26] V. Nava, M. Rajic, C. G. Soares, Effects of the mooring line configuration on the dynamics of a point absorber, in: ASME 2013 32nd International Conference on Ocean, Offshore and Arctic Engineering, American Society of Mechanical Engineers, pp. V008T09A071–V008T09A071.

[27] H. G. Zaroudi, K. Rezanejad, C. G. Soares, Assessment of mooring configurations on the performance of a floating oscillating water column energy converter, Taylor & Francis Group, London, 2015, book section Mooring Systems, pp. 921–928.

[28] D. V. Evans, Maximum wave-power absorption under motion constraints, Applied Ocean Research 3 (4) (1981) 200–203. doi:10.1016/0141-1187(81)90063-8.

[29] D. Pizer, Numerical modelling of wave energy absorbers, Report, University of Edinburgh (1994).

[30] J. Falnes, J. Hals, Heaving buoys, point absorbers and arrays, Philosophical Transactions of the Royal Society A: Mathematical, Physical and Engineering Sciences 370 (1959) (2012) 246–277. doi:10.1098/rsta.2011.0249.

[31] C. M. Linton, Radiation and diffraction of water waves by a submerged sphere in finite depth, Ocean Engineering 18 (12) (1991) 61–74. doi:10.1016/0029-8018(91)90034-N.

[32] S. Jiang, Y. Gou, B. Teng, D. Ning, Analytical solution of a wave diffraction problem on a submerged cylinder, Journal of Engineering Mechanics 140 (1) (2014) 225–232. doi:10.1061/(ASCE)EM.1943-7889.0000637.

[33] S. Jiang, Y. Gou, B. Teng, Water wave radiation problem by a submerged cylinder, Journal of Engineering Mechanics 140 (5) (2014) 06014003. doi:10.1061/(ASCE)EM.1943-7889.0000723.